

Top quark forward-backward asymmetry, FCNC decays and like-sign pair production as a joint probe of new physics

BY JUNJIE CAO¹, LIN WANG^{1,2}, LEI WU², JIN MIN YANG²

July 16, 2018

Abstract

Some extensions of the Standard Model often predict a Z' gauge boson which mediates flavor-changing neutral-current (FCNC) interaction between up and top quarks. These new physics models are phenomenologically attractive because they can explain the top quark forward-backward asymmetry A_{FB}^t measured recently by the Tevatron collider. In addition, they will induce the top quark FCNC decays and the like-sign top pair production which can be explored at the LHC. In this work we focus on two such models (the left-right model and the $U(1)_X$ model) to investigate their correlated effects on A_{FB}^t , the FCNC decays $t \rightarrow u V$ ($V = g, Z, \gamma$) and the like-sign top pair production at the LHC. We also pay special attention on the most recently measured A_{FB}^t in the large invariant mass region. We find that under the current experimental constraints both models can alleviate the deviation of A_{FB}^t and, meanwhile, enhance some FCNC decays and the like-sign pair production to the accessible level of the LHC. Further, since the two models give different predictions (for each observable and also for the correlation shape between different observables), they may even be distinguished by jointly studying these top quark observables.

1 INTRODUCTION

Since the top quark has a mass at weak scale and is the heaviest fermion in the Standard Model (SM), the top quark physics is speculated to be a sensitive probe for new physics beyond the SM [top-review-th]. So far the Tevatron collider has measured many properties of the top quark and found good agreement with the SM predictions except for the forward-backward asymmetry A_{FB}^t in the top pair production which shows about 2σ deviation from the theoretical expectation [top-afb-exp1]. Although the latest analysis based on the 5.3 fb^{-1} luminosity reduced the deviation of the CDF result

to about 1.8σ , it indicated that A_{FB}^t is dependent on the invariant mass ($M_{t\bar{t}}$) and for the high invariant mass region ($M_{t\bar{t}} \geq 450$ GeV) the deviation is enlarged to more than 3σ [top-afb-exp2].

Such a A_{FB}^t deviation reported by the Tevatron has recently stimulated many theorists to try to give an explanation in various new physics models [top-afb-th1, top-afb-th2, top-afb-th3, top-afb-th4], among which some frameworks predict a Z' gauge boson mediating FCNC interactions between up and top quarks [top-afb-th3, top-afb-th4]. Such Z' -models are especially interesting because, in addition to contributing to A_{FB}^t , they can simultaneously induce the top quark FCNC decays and the like-sign top pair production. As is well known, the FCNC interactions for the top quark in the SM are extremely suppressed [fcnc-sm] and any observation of top quark FCNC processes will serve as an unambiguous evidence for new physics. The like-sign top pair production is also a good probe for new physics because it gives two isolated like-sign leptons in the final states and is free from the $t\bar{t}$ background and the huge QCD W +jets background [like-sign top-th1, like-sign top-th2, like-sign top-th3]. Therefore, these different observables jointly can serve as a powerful probe for such Z' -models. Further, since these observables are correlated in a given model and the correlation behavior may be model-dependent, the models may even be distinguished by jointly studying these top quark observables. In this work we study such correlated observables in two different Z' -models: the left-right model and the $U(1)_X$ model. For the like-sign top pair production we focus on the process at the LHC (in our study the charge conjugate channel, i.e., the production of $\bar{t}\bar{t}$ is also included), while for the top quark FCNC processes we focus on the FCNC decays $t \rightarrow u V$ ($V = g, Z, \gamma$). For A_{FB}^t we will display the total asymmetry and the invariant mass dependent asymmetry.

This work is organized as follows. In Sec. II we briefly describe the two models and give the calculations for the observables. In Sec. III we present the numerical results and give some discussions. Finally, the conclusion is drawn in Sec. IV.

2 Models and Calculations

The extra gauge boson Z' is usually predicted in the extensions of the SM with an enlarged gauge group. In general, these models can be classified into two categories. One kind of models predict a family universal Z' which mediates the s -channel $t\bar{t}$ production and does not have significant effect on A_{FB}^t . The other kind of models predict a non-universal Z' with FCNC top quark couplings (say $Z' t \bar{u}$) which induces the t -channel $t\bar{t}$ production and may contribute to A_{FB}^t sizably. Since we attempt to explain A_{FB}^t by new physics effects, we focus on the following two models which predict a non-

universal Z' :

- (i) Model I is a $U(1)_X$ model [top-afb-th3]. With an additional $U(1)_X$ gauge symmetry, this model predicts a new gauge boson Z' which mediates FCNC interaction between the up and top quarks:

$$\mathcal{L}_{Z'} = g_x \bar{u} \gamma^\mu P_R t Z'_\mu + \epsilon_U g_x \bar{u}_i \gamma^\mu P_R u_i Z'_\mu \quad (1)$$

where $g_x (\alpha_x = g_x^2 / 4\pi)$ and ϵ_U are coupling constants. Since such interactions are only for the right-handed quarks, they can safely escape the low energy flavor constraints [top-afb-th2, top-afb-th3]. Note that the second term is a flavor diagonal interaction so the gauge boson Z' can have decay modes $Z' \rightarrow u_i \bar{u}_i$ which can suppress the like-sign top pair production proceeding through $u \bar{u} \rightarrow Z' Z'$ followed by $Z' \rightarrow t \bar{u}$ at the Tevatron [like-sign top-ep1]. The chiral gauge anomalies in this model can be avoided by introducing two sets of new heavy fermions [top-afb-th3].

- (ii) Model II is a left-right symmetric model [hexg]. This kind of left-right symmetric models are well motivated by the explanation of parity violation and neutrino masses. Here we focus on a special left-right symmetric model called the third-generation enhanced left-right model, which is based on the gauge group $SU(3)_C \times SU(2)_L \times SU(2)_R \times U(1)_{B-L}$ with gauge couplings g_3 , g_L , g_R and g respectively. The key feature of this model is that the gauge bosons of $SU(2)_R$ couple only to the third-generation fermions and allow for FCNC interaction at tree level [hexg, top-afb-th4]. In our analysis, we only consider the potentially large contribution from the neutral gauge interactions, which are given by

$$\begin{aligned} \mathcal{L}_{Z, Z'} = & -\frac{g_L}{2 \cos \theta_W} \bar{q} \gamma^\mu (g_V - g_A \gamma_5) q (\cos \xi_Z Z_\mu - \sin \xi_Z Z'_\mu) \\ & + \frac{g_Y}{2} \tan \theta_R \left(\frac{1}{3} \bar{q}_L \gamma^\mu q_L + \frac{4}{3} \bar{u}_{Ri} \gamma^\mu u_{Ri} - \frac{2}{3} \bar{d}_{Ri} \gamma^\mu d_{Ri} \right) (\sin \xi_Z Z_\mu + \cos \xi_Z Z'_\mu) \\ & - \frac{g_Y}{2} (\tan \theta_R + \cot \theta_R) (\bar{u}_{Ri} \gamma^\mu V_{Ri}^{u*} V_{Ri}^u u_{Rj} - \bar{d}_{Ri} \gamma^\mu V_{Ri}^{d*} V_{Ri}^d d_{Rj}) (\sin \xi_Z Z_\mu + \cos \xi_Z Z'_\mu) \end{aligned} \quad (2)$$

where $\tan \theta_R = g / g_R$, $g_Y = g \cos \theta_R = g_R \sin \theta_R$, ξ_Z is the mixing angle between Z_R and Z_0 , $V_{Rij}^{u,d}$ are the unitary matrices which rotate the right-handed quarks u_{Ri} and d_{Ri} from interaction basis to mass eigenstates and the repeated generation indices i and j are summed. If $g_R \gg g_Y$ or equally $\cot \theta_R \gg 1$, we can see that the $Z' \bar{u}_{iR} u_{jR}$ interaction will become strong. Note that a sizable $u_R - t_R$ mixing with other flavor mixings suppressed can still avoid the severe low energy

constraints [top-afb-th3], which is similar to model I. About the parameters ξ_Z and $m_{Z'}$ in this model, the oblique T parameter and perturbative requirement will give constraints on ξ_Z (versus $m_{Z'}$) [hexg]. However, such constraints are obtained under the requirement to explain the b -quark forward-backward asymmetry A_{FB}^b , which, of course, can be relaxed if we give up the explanation of A_{FB}^b . Furthermore, for the $t\bar{t}$ and like-sign top pair productions, the main contributions are independent of the parameter ξ_Z [top-afb-th4]. Therefore, the constraints from the T parameter are almost irrelevant to our numerical study. We note that the constraints from CDF search for Z' and from the global fitting of the electroweak precision data are invalid here since these constraints arise mostly from the processes involving the first- or second-generation of fermions. So far the pertinent bound comes from $e^+e^- \rightarrow b\bar{b}$ at LEP-II, which requires $M_{Z'} \gtrsim 460$ GeV for $\cot \theta_R \geq 10$.

As shown in Fig.1, both models can contribute to the $t\bar{t}$ production and thus subject to the constraints from the measurements of the cross section and invariant mass distribution at the Tevatron [cross section, mtt]. Note that the t – channel diagram in Fig.1 can interfere with the QCD process, which may sizably alter the $t\bar{t}$ production rate and also make significant contribution to A_{FB}^t . The analytic results for these processes are available in [top-afb-th2, top-afb-th4].

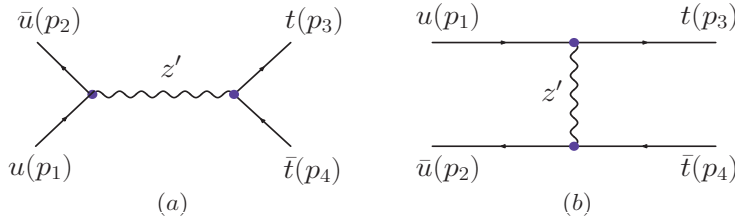


Figure 1. Feynman diagrams contributing to $t\bar{t}$ production.

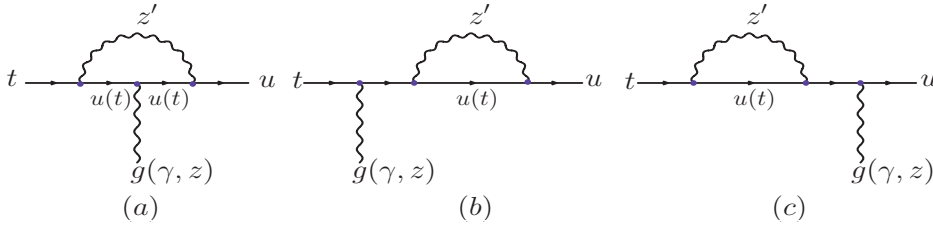


Figure 2. The loop diagrams contributing to $t \rightarrow u V$ ($V = g, Z, \gamma$).

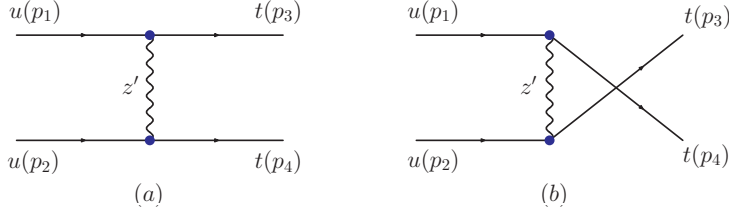


Figure 3. Feynman diagrams contributing to $t\bar{t}$ production.

As shown in Fig.2, at loop level both models can induce the top quark FCNC decays $t \rightarrow u V$ ($V = g, Z, \gamma$). Note that in model II the decay mode $t \rightarrow u Z$ can occur at tree level. The amplitudes of all the loop diagrams are listed in the Appendix. Of course, if Z' is much lighter than the top quark, the rare decay $t \rightarrow u Z'$ can be also open, which may cause the tension between the measurements of dilepton and lepton+jets channels for $t\bar{t}$ production. In additional, a recent CDF measurement for the events of like-sign dilepton plus b-jets severely constrained the heavy mass region of Z' . In our calculation we take $m_{Z'}$ from 120 GeV to 170 GeV to evade such constraints [top-afb-th3].

Both models can induce the like-sign top pair production, as depicted in Fig.3. Such a production has been studied in [top-afb-th2, like-sign top-th3]. In our study we consider its correlation with A_{FB}^t and the top quark FCNC decays. There are other channels for like-sign top pair productions, such as $u g \rightarrow t Z' \rightarrow t t \bar{u}$ and $u \bar{u} \rightarrow Z' Z' \rightarrow t \bar{u} t \bar{u}$, which, however, are suppressed both kinematically and by high order FCNC couplings at the LHC.

3 Numerical results and discussions

To be consistent with the mass of top quark used in the measurements, we choose $m_t = 172.5$ GeV. Other SM parameters used in our numerical calculation are [pdg]

$$m_Z = 91.19 \text{ GeV}, \sin^2 \theta_W = 0.2228, \alpha_s(m_t) = 0.1095, \alpha = 1/128. \quad (3)$$

Considering the experimental constraints, we scan the new physics parameters in the following ranges for model I and model II:

$$\text{Model I: } 120 \text{ GeV} < m_{Z'} < 170 \text{ GeV}, 0.05 < \epsilon_U < 0.1, 0 < \alpha_x < 0.05;$$

Model II: $500 \text{ GeV} < m_{Z'} < 2000 \text{ GeV}$, $10 < \cot \theta < 20$, $0.1 < (V_R^u)_{ut} < 0.2$, $0 < \xi_Z < 0.02$.

In the calculation we use the CTEQ6L parton distribution function [cteq] and the renormalization scale μ_R and factorization scale μ_F are chosen to be $\mu_R = \mu_F = m_t$. Due to the interference of the FCNC t -channel diagram with the SM QCD diagram, we require the total cross section and the differential cross section in each bin to be within the 2σ regions of their experimental values [cross section, mtt].

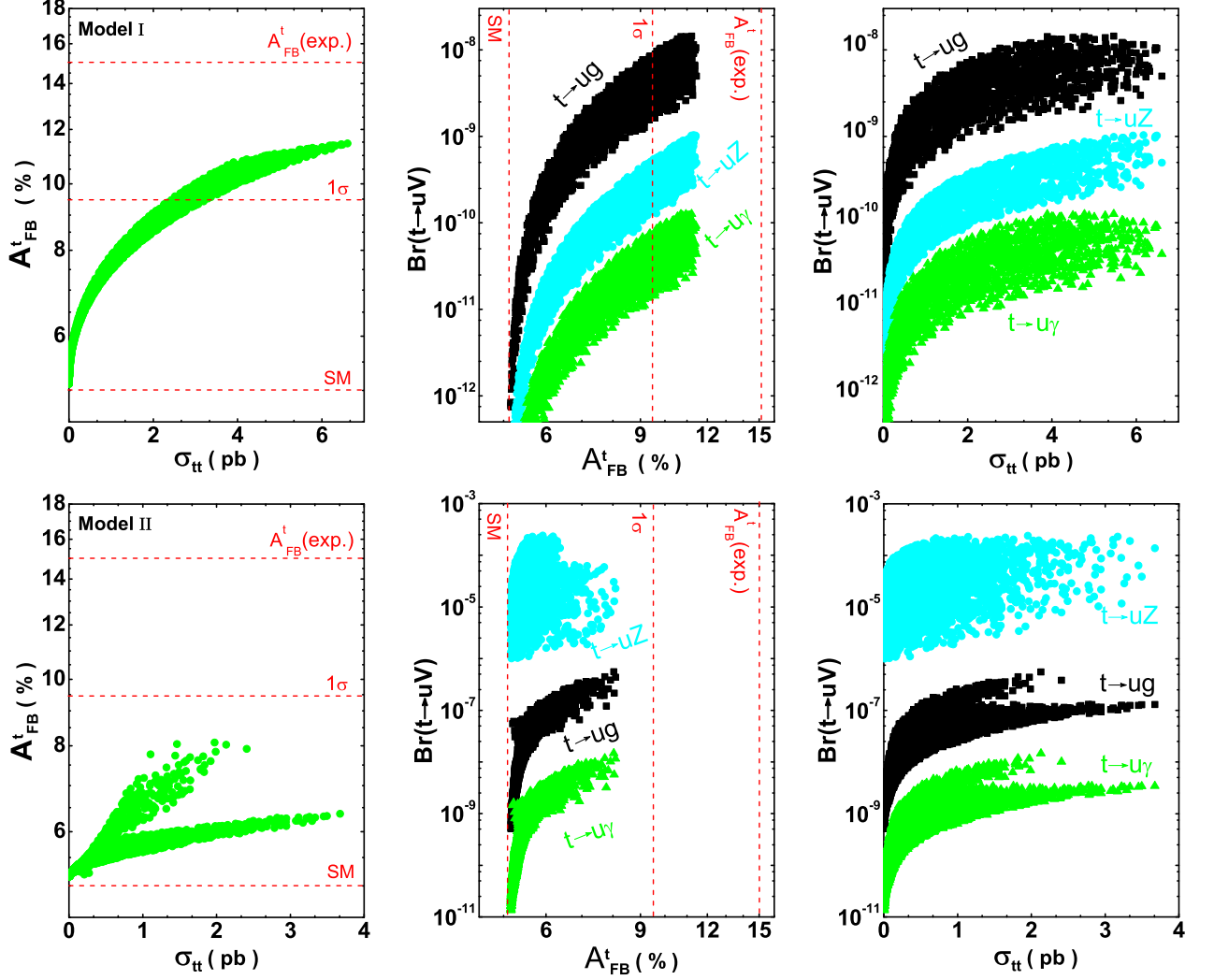


Figure 4. The correlations between A_{FB}^t at the Tevatron, the branch ratio of top FCNC decays and the cross section of the like-sign top pair production at the LHC with $\sqrt{s} = 14 \text{ TeV}$.

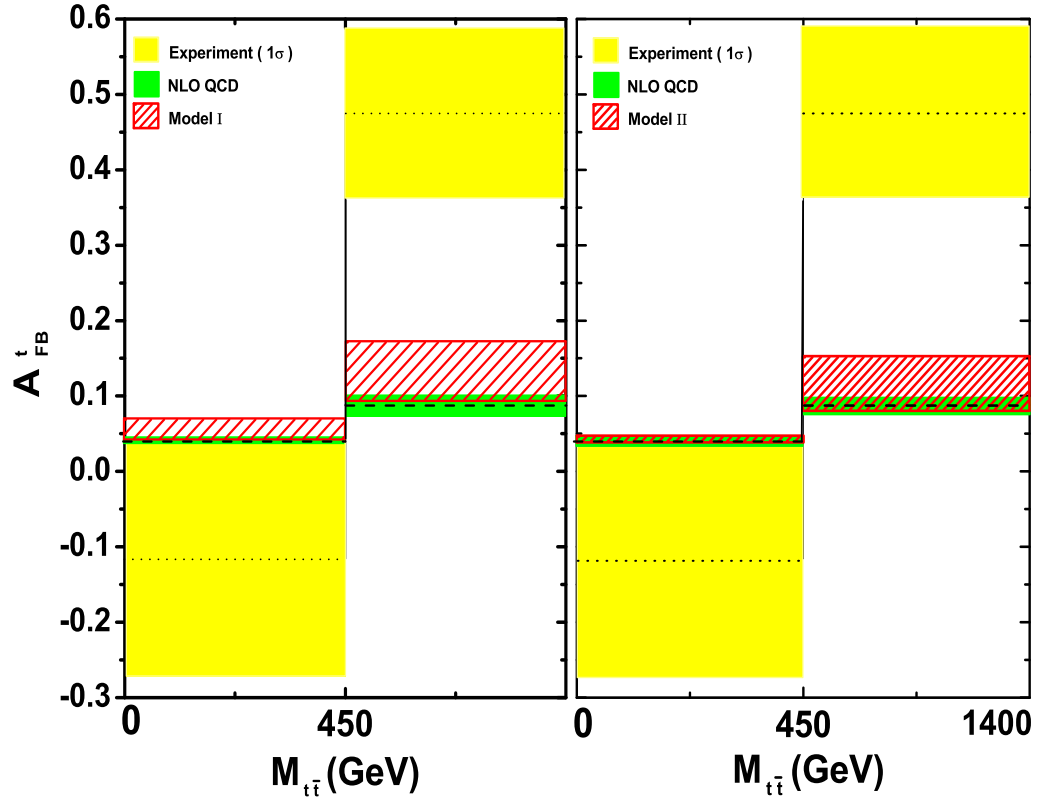


Figure 5. Top quark forward-backward asymmetry at the Tevatron versus $t\bar{t}$ invariant mass.

For each model, we show in Fig.4 the correlations between the A_{FB}^t at the Tevatron, the branch ratios of top FCNC decays and the cross section of the like-sign top pair production at the LHC with $\sqrt{s} = 14\text{TeV}$. We see that for A_{FB}^t each model can improve the theoretical prediction, allaying the deviation from the experimental value. Especially, for model I the theoretical prediction of A_{FB}^t can be improved to agree with the experimental value at 1σ level. Since the new t -channel contributions will modify the $t\bar{t}$ invariant mass distribution, we further investigate their effects on the mass-dependent A_{FB}^t which is measured by CDF recently. In the calculation of A_{FB}^t , we multiply a K-factor (~ 1.31) [k-factor] to normalize the total cross section in the SM to the NLO value. From Fig.5 we see that each model can enhance the theoretical value of A_{FB}^t in the large invariant mass region and ameliorate the deviation from the experimental data. But still the deviation remains larger than 2σ .

For the top FCNC decays, the present experimental bounds are still weak, such as $Br(t \rightarrow u g) < 0.02\%$ from D0 [tug], $Br(t \rightarrow u \gamma) < 0.75\%$ from ZEUS [tur], $Br(t \rightarrow u Z) < 3.7\%$ from CDF [tuz]. From Fig.4 we see that the branch ratios of these processes in the two models are far below the current upper bounds and unlikely to reach the sensitivity of the LHC ($\sim O(10^{-6})$) [top-review-th]) except for the decay $t \rightarrow u Z$ in model II which occurs at tree level and thus can be quite large. Actually, although these FCNC decays are usually greatly enhanced in the popular new physics models such as low energy supersymmetry [fcnc-susy], technicolor [fcnc-tc] or little Higgs theory [fcnc-lh], detecting such rare decays at the LHC is still quite challenging. For the like sign top pair production, we see from Fig.4 that the maximal production rate at the LHC can reach 6.8 pb for model I and 3.7 pb for model II, which, as discussed below, could be detectable at the LHC. Note that both models could also cause sizable top polarization asymmetry in $t\bar{t}$ production at the LHC [top-afb-th2, wulei].

The different observables are correlated in a given model, as shown in Fig.4. The correlation shapes are quite different for the two models. Further, as shown in Fig.6, some kinematical distributions (the top quark transverse momentum p_T^t and its pseudo-rapidity η_t , the total transverse energy H_T of the process and the separation between the two b -jets $\Delta R_{bb} \equiv \sqrt{(\Delta\phi)^2 + (\Delta\eta)^2}$) for the like-sign top pair production at the LHC are

also quite different for the two models due to their different values of $M_{Z'}$. All these differences may be useful for distinguishing the models.

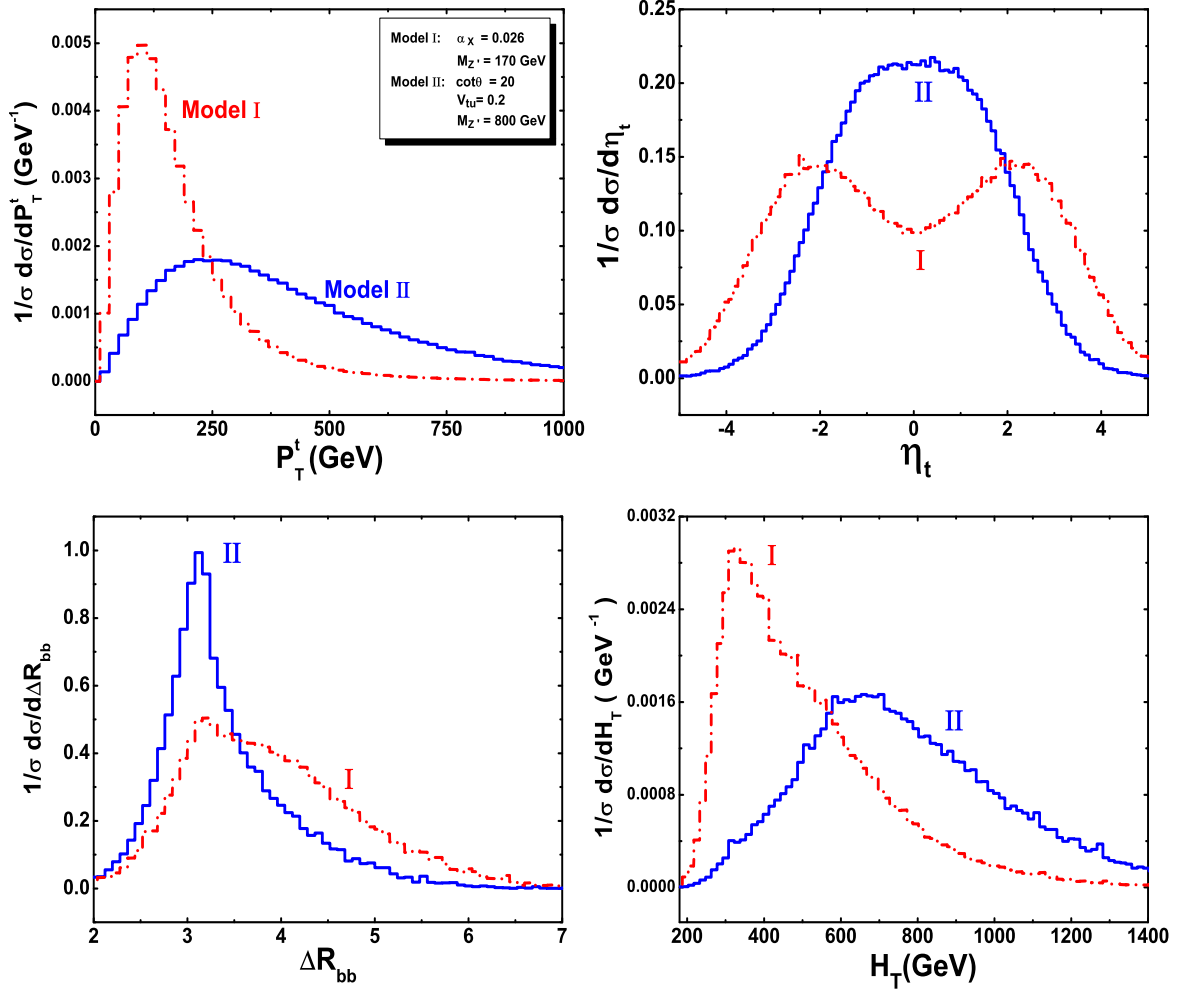


Figure 6. The p_T^t , η_t , ΔR_{bb} and H_T distributions for the like sign top pair production at the LHC.

Now we study the observability of the like-sign top pair production at the LHC. The like-sign top pair can be identified as a same-charge lepton pair

plus b -jets. To be more realistic, we simulate the energy resolution of the detector effects by assuming a Gaussian smearing for the final leptons and jets [energy resolution]

$$\frac{\Delta E}{E} = \frac{5\%}{\sqrt{E}} \oplus 0.55\%, \quad \text{for leptons;} \quad (4)$$

$$\frac{\Delta E}{E} = \frac{100\%}{\sqrt{E}} \oplus 5\% \quad \text{for jets ;} \quad (5)$$

where E is in GeV, and \oplus indicates that the energy-dependent and energy-independent terms are added in quadrature. Furthermore, we take the b -jet tagging efficiency as 50%. The main backgrounds are from $qq' \rightarrow t\bar{t}W^\pm$ and $qq \rightarrow W^\pm q' W^\pm q'$, which have been studied in [like-sign top-th2]. In our analysis we take the same cuts as in [like-sign top-th2] for the signal:

$$\begin{aligned} p_T^\ell &> 15 \text{ GeV}, E_T^j > 40 \text{ GeV}, |\eta_\ell|, |\eta_j| < 2.5, \Delta R_{\ell j}, \Delta R_{jj} > 0.4 \\ M(\ell_1 j_1), M(\ell_2 j_2) &< 160 \text{ GeV}, M(\ell\ell jj) > 500 \text{ GeV} \end{aligned} \quad (6)$$

Here E_T denotes the transverse energy and M is the invariant mass of the final states. Note that the numerical results displayed in Figs.4 and 6 for the like-sign top pair production were obtained with the above kinematic cuts. From the ΔR_{bb} distribution in Fig. 6 we see that the distribution exhibits a peak at large ΔR_{bb} (near $\theta_{bb} = \pi$) because the two b -jets come from the back-to-back top pair and they are expected to fly into the opposite directions. Compared with model I, the heavier Z' in model II will produce the more energetic lepton and jet, and then lead to the larger H_T and p_T . It is also interesting to notice that the pseudo-rapid distribution shows two peaks for model I and one peak for model II.

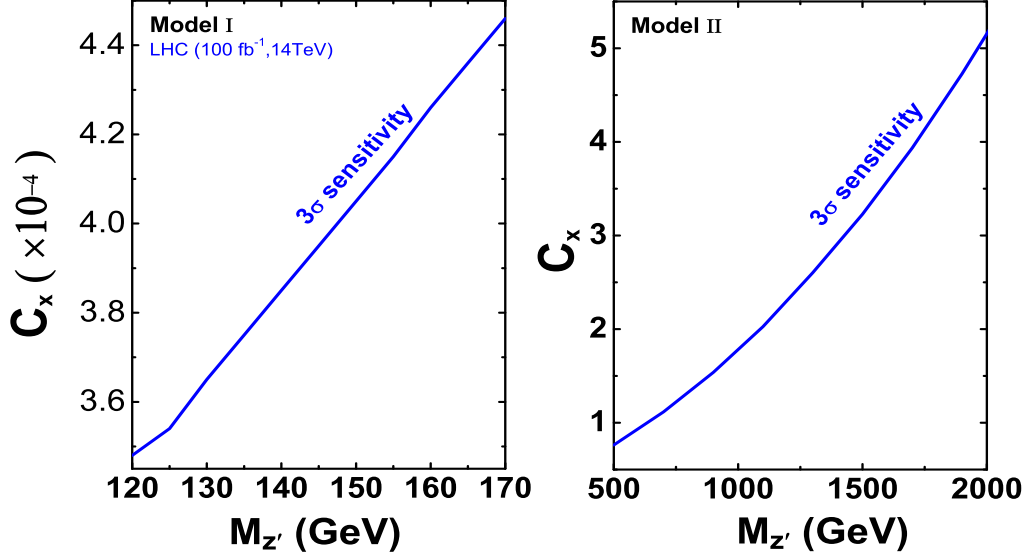


Figure 7. The 3σ sensitivity contour for the like sign top pair at the LHC. The region above each curve is the corresponding 3σ observable region. Here C_x 's denote respectively α_x and $V_{tu}^2 (\cot \theta + \tan \theta)^2$ for model I and model II.

Combining our signal calculation with the background calculation in [like-sign top-th2], we in Fig.7 plot the 3σ sensitivity for the like-sign top pair production at the LHC with a luminosity of 100 fb^{-1} , where the region above each curve is the corresponding observable region. We see that for each model there are still a large parameter space in which the like-sign top pair production can be above the 3σ sensitivity of the LHC.

4 conclusion

We studied the correlated effects on A_{FB}^t at the Tevatron, the FCNC decays $t \rightarrow u V$ ($V = g, Z, \gamma$) and the like-sign top pair production at the LHC in two new physics models: the left-right model and the $U(1)_X$ model. For A_{FB}^t we also investigated its mass dependent predictions and compared with the recent CDF results. The deviation of the mass dependent A_{FB}^t is found to be improved in both models. For each model the production rate of the like-sign top pair at the LHC can be large and accessible in a large parameter space. Further, since these two models give different predictions for each observable and also for the correlation between different observables, these top quark observables may be useful for distinguishing the different models.

Acknowledgement

This work was supported in part by HASTIT under grant No. 2009HASTIT004, by the National Natural Science Foundation of China (NNSFC) under grant Nos. 10821504, 10725526, 10775039, 11075045 and by the Project of Knowledge Innovation Program (PKIP) of Chinese Academy of Sciences under grant No. KJCX2.YW.W10.

5 Analytic expressions for FCNC decay amplitudes

Here we list the loop amplitude expressions for the processes $t \rightarrow u V$ ($V = g, \gamma, Z$) shown in Fig.2 for model I and model II. The notation (u, t) represents the u, t quark appearing respectively in the propagators.

For model I the amplitudes are given by

$$\mathcal{M}_g^{(a)}(u, t) = a g_s T_{\beta\alpha}^A \bar{u}(p_u) [-4 C^{1\nu\rho} \gamma_\rho - \gamma^\nu + 2 B_0^1 \gamma^\nu - 2 (\text{slashed}) p_t - (\text{slashed}) p_u] \gamma^\nu \gamma^\rho C_\rho^1 P_R u(p_t) \varepsilon_\nu^*(p_g) \quad (7)$$

$$\mathcal{M}_g^{(b)}(u, t) = a g_s T_{\beta\alpha}^A \bar{u}(p_u) \frac{(2 B_1^2 + 1) m_t (\text{slashed}) p_u \gamma^\nu P_L}{p_u^2 - m_t^2} u(p_t) \varepsilon_\nu^*(p_g) \quad (8)$$

$$\mathcal{M}_g^{(c)}(u, t) = a g_s T_{\beta\alpha}^A \bar{u}(p_u) \frac{(2 B_1^3 + 1) m_t^2 \gamma^\nu P_R}{p_t^2 - m_u^2} u(p_t) \varepsilon_\nu^*(p_g) \quad (9)$$

$$\mathcal{M}_\gamma^{(a)}(u, t) = \frac{2}{3} e a \bar{u}(p_u) [-4 C^{2\nu\rho} \gamma_\rho - \gamma^\nu + 2 B_0^4 \gamma^\nu - 2 (\text{slashed}) p_t - (\text{slashed}) p_u] \gamma^\nu \gamma^\rho C_\rho^2 P_R u(p_t) \varepsilon_\nu^*(p_\gamma) \quad (10)$$

$$\mathcal{M}_\gamma^{(b)}(u, t) = \frac{2}{3} e a \bar{u}(p_u) \frac{(2 B_1^5 + 1) m_t (\text{slashed}) p_u \gamma^\nu P_L}{p_u^2 - m_t^2} u(p_t) \varepsilon_\nu^*(p_\gamma) \quad (11)$$

$$\mathcal{M}_\gamma^{(c)}(u, t) = \frac{2}{3} e a \bar{u}(p_u) \frac{(2 B_1^6 + 1) m_t^2 \gamma^\nu P_R}{p_t^2 - m_u^2} u(p_t) \varepsilon_\nu^*(p_\gamma) \quad (12)$$

$$\mathcal{M}_Z^{(a)}(u) = -a \delta_{\alpha\beta} g \bar{u}(p_u) \left(\frac{2}{3} \sin \theta_W \tan \theta_W \right) [-4 C^{3\nu\rho} \gamma_\rho - \gamma^\nu + 2 B_0^7 \gamma^\nu - 2 (\text{slashed}) p_t - (\text{slashed}) p_u] \gamma^\nu \gamma^\rho C_\rho^3 P_R u(p_t) \varepsilon_\nu^*(p_Z) \quad (13)$$

$$\mathcal{M}_Z^{(a)}(t) = -a \delta_{\alpha\beta} g \bar{u}(p_u) \left[\frac{m_t^2}{\cos \theta_W} C_0^4 \gamma^\nu P_R + \frac{2}{3} \sin \theta_W \tan \theta_W \left[-4 C^{4\nu\rho} \gamma_\rho - \gamma^\nu + 2 B_0^8 \gamma^\nu - 2 (\text{slashed}) p_t - (\text{slashed}) p_u \right] \gamma^\nu \gamma^\rho C_\rho^4 P_R \right] u(p_t) \varepsilon_\nu^*(p_Z) \quad (14)$$

$$\mathcal{M}_Z^{(b)}(u, t) = -a \delta_{\alpha\beta} g \bar{u}(p_u) \left(\frac{4 \sin^2 \theta_W - 3}{6 \cos \theta_W} \right) \left[\frac{(2 B_1^9 + 1) m_t (\text{slashed}) p_u \gamma^\nu P_L}{p_u^2 - m_t^2} \right] u(p_t) \varepsilon_\nu^*(p_Z) \quad (15)$$

$$\mathcal{M}_Z^{(c)}(u, t) = -a \delta_{\alpha\beta} g \bar{u}(p_u) \left(\frac{2}{3} \sin \theta_W \tan \theta_W \right) \frac{(2 B_1^{10} + 1) m_t^2 \gamma^\nu P_R}{p_t^2 - m_u^2} u(p_t) \varepsilon_\nu^*(p_Z), \quad (16)$$

where p_t and p_u denote respectively the momenta of the top and up quark, and the loop functions B and C are defined in [loop] and use LoopTools [Hahn] in the calculations.

The loop functions' dependence on the momentum and mass is given by

$$\begin{aligned}
B^1(u) &= B(p_t, m_{Z'}, m_u), & B^1(t) &= B(p_t, m_{Z'}, m_t), & B^2(u) &= B(-p_u, m_u, m_{Z'}), \\
B^2(t) &= B(-p_u, m_t, m_{Z'}), & B^3(u) &= B(-p_t, m_u, m_{Z'}), & B^3(t) &= B(-p_t, m_t, m_{Z'}), \\
B^4(u) &= B(p_t, m_{Z'}, m_u), & B^4(t) &= B(p_t, m_{Z'}, m_t), & B^5(u) &= B(-p_u, m_u, m_{Z'}), \\
B^5(t) &= B(-p_u, m_t, m_{Z'}), & B^6(u) &= B(-p_t, m_u, m_{Z'}), & B^6(t) &= B(-p_t, m_t, m_{Z'}), \\
B^7(u) &= B(p_t, m_{Z'}, m_u), & B^8(t) &= B(p_t, m_{Z'}, m_t), & B^9(u) &= B(-p_u, m_u, m_{Z'}), \\
B^9(t) &= B(-p_u, m_t, m_{Z'}), & B^{10}(u) &= B(-p_t, m_u, m_{Z'}), & B^{10}(t) &= B(-p_t, m_t, m_{Z'})
\end{aligned}$$

$$\begin{aligned}
C^1(u) &= C(-p_u, p_t, m_u, m_{Z'}, m_u), & C^1(t) &= C(-p_u, p_t, m_t, m_{Z'}, m_t), \\
C^2(u) &= C(-p_u, p_t, m_u, m_{Z'}, m_u), & C^2(t) &= C(-p_u, p_t, m_t, m_{Z'}, m_t), \\
C^3(u) &= C(-p_u, p_t, m_u, m_{Z'}, m_u), & C^4(t) &= C(-p_u, p_t, m_t, m_{Z'}, m_t).
\end{aligned}$$

For model II the amplitudes are given by

$$\mathcal{M}_g^{(a)}(u) = b \ g_s \ T_{\beta\alpha}^A \ \bar{u}(p_u) [-4 \ C^{1\nu\rho} \ \gamma_\rho - \gamma^\nu + 2 \ B_0^1 \ \gamma^\nu - 2 \ (\text{slashed}) p_t - (\text{slashed}) p_u] \gamma^\nu \gamma^\rho C_\rho^1 g_{Z'R}^u P_R u(p_t) \varepsilon_\nu^*(p_g) \quad (17)$$

$$\begin{aligned}
\mathcal{M}_g^{(a)}(t) &= b \ g_s \ T_{\beta\alpha}^A \ \bar{u}(p_u) \{ [-4 \ C^{2\nu\rho} \ \gamma_\rho - \gamma^\nu + 2 \ B_0^2 \ \gamma^\nu - 2 \ (\text{slashed}) p_t - (\text{slashed}) p_u] \gamma^\nu \gamma^\rho C_\rho^2 g_{Z'R}^t P_R \\
&\quad + 8 m_t C^{2\nu} g_{Z'L}^t P_L - 4 m_t (p_u - p_t)^\nu C_0^2 g_{Z'L}^t P_L \} u(p_t) \varepsilon_\nu^*(p_g) \quad (18)
\end{aligned}$$

$$\mathcal{M}_g^{(b)}(u) = b g_s T_{\beta\alpha}^A \bar{u}(p_u) \frac{(2 B_1^3 + 1) m_t (\text{slashed}) p_u \gamma^\nu g_{Z'R}^u P_L}{p_u^2 - m_t^2} u(p_t) \varepsilon_\nu^*(p_g) \quad (19)$$

$$\begin{aligned}
\mathcal{M}_g^{(b)}(t) &= b \ g_s \ T_{\beta\alpha}^A \ \bar{u}(p_u) \{ (2 B_1^4 + 1) \ m_t (\text{slashed}) p_u \ \gamma^\nu \ g_{Z'R}^t P_L + (4 B_0^4 - 2) m_t (\text{slashed}) p_u \gamma^\nu g_{Z'L}^t P_L \\
&\quad + (4 B_0^4 - 2) m_t^2 \gamma^\nu g_{Z'L}^t P_R \} \frac{u(p_t) \varepsilon_\nu^*(p_g)}{p_u^2 - m_t^2} \quad (20)
\end{aligned}$$

$$\mathcal{M}_g^{(c)}(u) = b g_s T_{\beta\alpha}^A \bar{u}(p_u) \frac{(2 B_1^5 + 1) m_t^2 \gamma^\nu g_{Z'R}^u P_R}{p_t^2 - m_u^2} u(p_t) \varepsilon_\nu^*(p_g) \quad (21)$$

$$\mathcal{M}_g^{(c)}(t) = b g_s T_{\beta\alpha}^A \bar{u}(p_u) \frac{(2 B_1^6 + 1) m_t^2 \gamma^\nu g_{Z'R}^t P_R + (4 B_0^6 - 2) m_t \gamma^\nu (\text{slashed}) p_t g_{Z'L}^t P_L}{p_t^2 - m_u^2} u(p_t) \varepsilon_\nu^*(p_g) \quad (22)$$

$$\begin{aligned}
\mathcal{M}_\gamma^{(a)}(u) &= \frac{2}{3} \ e \ b \ \bar{u}(p_u) [-4 \ C^{3\nu\rho} \ \gamma_\rho - \gamma^\nu + 2 \ B_0^7 \ \gamma^\nu - 2 \ (\text{slashed}) p_t - (\text{slashed}) p_u] \gamma^\nu \gamma^\rho C_\rho^3 g_{Z'R}^u P_R u(p_t) \varepsilon_\nu^*(p_\gamma) \quad (23)
\end{aligned}$$

$$\begin{aligned}
\mathcal{M}_\gamma^{(a)}(t) &= \frac{2}{3} \ e \ b \ \bar{u}(p_u) \{ [-4 \ C^{4\nu\rho} \ \gamma_\rho - \gamma^\nu + 2 \ B_0^8 \ \gamma^\nu - 2 \ (\text{slashed}) p_t - (\text{slashed}) p_u] \gamma^\nu \gamma^\rho C_\rho^4 g_{Z'R}^t P_R \\
&\quad + 8 m_t C^{4\nu} g_{Z'L}^t P_L - 4 m_t (p_u - p_t)^\nu C_0^4 g_{Z'L}^t P_L \} u(p_t) \varepsilon_\nu^*(p_\gamma) \quad (24)
\end{aligned}$$

$$\mathcal{M}_\gamma^{(b)}(u) = \frac{2}{3} \ e \ b \ \bar{u}(p_u) \frac{(2 B_1^9 + 1) m_t (\text{slashed}) p_u \gamma^\nu g_{Z'R}^u P_L}{p_u^2 - m_t^2} u(p_t) \varepsilon_\nu^*(p_\gamma) \quad (25)$$

$$\begin{aligned}
\mathcal{M}_\gamma^{(b)}(t) &= \frac{2}{3} \ e \ b \ \bar{u}(p_u) \{ (2 B_1^{10} + 1) \ m_t (\text{slashed}) p_u \ \gamma^\nu \ g_{Z'R}^t P_L + (4 B_0^{10} - 2) m_t (\text{slashed}) p_u \gamma^\nu g_{Z'L}^t P_L \\
&\quad + (4 B_0^{10} - 2) m_t^2 \gamma^\nu g_{Z'L}^t P_R \} \frac{u(p_t) \varepsilon_\nu^*(p_\gamma)}{p_u^2 - m_t^2} \quad (26)
\end{aligned}$$

$$\mathcal{M}_\gamma^{(c)}(u) = \frac{2}{3} \ e \ b \ \bar{u}(p_u) \frac{(2 B_1^{11} + 1) m_t^2 \gamma^\nu g_{Z'R}^u P_R}{p_t^2 - m_u^2} u(p_t) \varepsilon_\nu^*(p_\gamma) \quad (27)$$

$$\begin{aligned}
\mathcal{M}_\gamma^{(c)}(t) &= \frac{2}{3} \ e \ b \ \bar{u}(p_u) \frac{(2 B_1^{12} + 1) m_t^2 \gamma^\nu g_{Z'R}^t P_R + (4 B_0^{12} - 2) m_t \gamma^\nu (\text{slashed}) p_t g_{Z'L}^t P_L}{p_t^2 - m_u^2} u(p_t) \varepsilon_\nu^*(p_\gamma), \\
&\quad (28)
\end{aligned}$$

where the loop function dependence is given by

$$\begin{aligned}
B^1(u) &= B(p_t, m_{Z'}, m_u), & B^2(t) &= B(p_t, m_{Z'}, m_t), & B^3(u) &= B(-p_u, m_u, m_{Z'}) \\
B^4(t) &= B(-p_u, m_t, m_{Z'}), & B^5(u) &= B(-p_t, m_u, m_{Z'}), & B^6(t) &= B(-p_t, m_t, m_{Z'}) \\
B^7(u) &= B(p_t, m_{Z'}, m_u), & B^8(t) &= B(p_t, m_{Z'}, m_t), & B^9(u) &= B(-p_u, m_u, m_{Z'}) \\
B^{10}(t) &= B(-p_u, m_t, m_{Z'}), & B^{11}(u) &= B(-p_t, m_u, m_{Z'}), & B^{12}(t) &= B(-p_t, m_t, m_{Z'})
\end{aligned}$$

$$\begin{aligned}
C^1(u) &= C(-p_u, p_t, m_u, m_{Z'}, m_u), & C^2(t) &= C(-p_u, p_t, m_t, m_{Z'}, m_t) \\
C^3(u) &= C(-p_u, p_t, m_u, m_{Z'}, m_u), & C^4(t) &= C(-p_u, p_t, m_t, m_{Z'}, m_t)
\end{aligned}$$

The constants in the above equations are given by

$$a = -\frac{i}{16\pi^2} \epsilon_\mu g_x^2, \quad (29)$$

$$b = \frac{i}{16\pi^2} \frac{e^2 V_{Rtu}^{u*} V_{Rtt}^u}{4 \cos^2 \theta_W \sin \theta_W} (\tan \theta_R + \cot \theta_R) \quad (30)$$

$$g_{Z'L}^{u,t} = (1 - \frac{4}{3} \sin^2 \theta_W) \xi + \frac{1}{3} \sin \theta_W \tan \theta_R, \quad (31)$$

$$g_{Z'R}^u = -\frac{4}{3} \sin^2 \theta_W \xi + \frac{4}{3} \sin \theta_W \tan \theta_R \quad (32)$$

$$g_{Z'R}^t = -\frac{4}{3} \sin^2 \theta_W \xi + \frac{1}{3} \sin \theta_W \tan \theta_R - \sin \theta_W \cot \theta_R \quad (33)$$

Bibliography

- [**top-review-th**] For top quark reviews, see, e.g., W. Bernreuther, [\(jfont\)](#)J. Phys. **G3**,5, 083001,(2008) D. Chakraborty, J. Konigsberg, D. Rainwater, *Ann. Rev. Nucl. Part. Sci.* **53**, 301 (2003); E. H. Simmons, hep-ph/0211335; C.-P. Yuan, hep-ph/0203088; S. Willenbrock, hep-ph/0211067; M. Beneke, *et al.*, hep-ph/0003033; T. Han, arXiv:0804.3178; For model-independent new physics study, see, e.g., C. T. Hill and S. J. Parke, [\(jfont\)](#)Phys. Rev. D **4**,9, 4454 (1994); K. Whisnant, *et al.*, [\(jfont\)](#)Phys. Rev. D **5**,6, 467 (1997); J. M. Yang, B.-L. Young, [\(jfont\)](#)Phys. Rev. D **5**,6, 5907 (1997); K. Hikasa, *et al.*, [\(jfont\)](#)Phys. Rev. D **5**,8, 114003 (1998); J. A. Aguilar-Saavedra, arXiv:0811.3842; R.A. Coimbra, *et al.*, arXiv:0811.1743.
- [**top-afb-exp1**] G. Stricker *et al.*, CDF note 9724 (2009); T. Aaltonen *et al.* [CDF Collaboration], Phys. Rev. Lett. **101**, 202001 (2008); V. M. Abazov *et al.* [D0 Collaboration], Phys. Rev. Lett. **100**, 142002 (2008).
- [**top-afb-exp2**] T. Aaltonen *et al.* [The CDF Collaboration], arXiv:1101.0034 [hep-ex].
- [**top-afb-th1**] A. Djouadi *et al.*, [\(jfont\)](#)Phys. Rev. D **8**,2, 071702 (2010); P. Ferrario, G. Rodrigo, [\(jfont\)](#)Phys. Rev. D **8**,0, 051701 (2009); K. Cheung, W. Y. Keung, T. C. Yuan, [\(jfont\)](#)Phys. Lett. B **6**,82, 287 (2009); S. Jung *et al.*, [\(jfont\)](#)Phys. Rev. D **8**,1, 015004 (2010); J. Shu, T. Tait, K. Wang, [\(jfont\)](#)Phys. Rev. D **8**,1, 034012 (2010); P. H. Frampton, J. Shu, K. Wang, [\(jfont\)](#)Phys. Rev. D **6**,83, 294 (2010); A. Arhrib, R. Benbrik, C. H. Chen, [\(jfont\)](#)Phys. Rev. D **8**,2, 034034 (2010); I. Dorsner *et al.*, [\(jfont\)](#)Phys. Rev. D **8**,1, 055009 (2010); D. W. Jung *et al.*, [\(jfont\)](#)Phys. Lett. B **6**,91, 238 (2010); V. Ahrens *et al.*, JHEP **1009**, 097 (2010); M. V. Martynov, A. D. Smirnov, Mod. Phys. Lett. A **25**, 2637 (2010); R. S. Chivukula, E. H. Simmons, C.-P. Yuan, [\(jfont\)](#)Phys. Rev. D **8**,2, 094009 (2010); Q.-H. Cao *et al.*, Phys. Rev. **D81**, 114004 (2010); G. Rodrigo and P. Ferrario, arXiv:1007.4328; V. Barger, W.-Y. Keung, C.-T. Yu, [\(jfont\)](#)Phys. Rev. D **8**,1, 113009 (2010); M. Bauer *et al.*, JHEP **1011**, 039 (2010); C. Zhang, S. Willenbrock, arXiv:1008.3869; J. A. Aguilar-Saavedra, [\(jfont\)](#)Nucl. Phys. B **8**,43, 638 (2011); C. H. Chen, G. Cvetič, C. S. Kim, arXiv:1009.4165; K. Kumar *et al.*, JHEP **1008**, 052 (2010); C. Degrande *et al.*, arXiv:1010.6304 [hep-ph]; B. Xiao, Y.-

- K. Wang, S. h. Zhu, [\(jnfnt\)Phys. Rev. D](#) **8**,2, 034026 (2010); arXiv:1011.0152; arXiv:1101.2507; G. Burdman, L. Lima, R. D. Matheus, arXiv:1011.6380; E. Alvarez, L. Rold, A. Szykman, arXiv:1011.6557; D. W. Jung *et al.*, arXiv:1012.0102; K. Cheung, T. C. Yuan, arXiv:1101.1445.
- [top-afb-th2]** D. W. Jung, P. Ko and J. S. Lee, arXiv:1011.5976; D. Choudhury *et al.*, arXiv:1012.4750.
- [top-afb-th3]** S. Jung, H. Murayama, A. Pierce and J. D. Wells, [\(jnfnt\)Phys. Rev. D](#) **8**,1, 015004 (2010).
- [top-afb-th4]** J. Cao *et al.*, [\(jnfnt\)Phys. Rev. D](#) **8**,1, 014016 (2010);
- [fcnc-sm]** G. Eilam, J. L. Hewett and A. Soni, [\(jnfnt\)Phys. Rev. D](#) **4**,4, 1473 (1991); B. Mele, S. Petrarca and A. Soddu, [\(jnfnt\)Phys. Lett. B](#) **4**,35, 401 (1998).
- [like-sign top-th1]** T. Stelzer, Z. Sullivan and S. Willenbrock, [\(jnfnt\)Phys. Rev. D](#) **5**,8, 094021 (1998); W. S. Hou *et al.*, [\(jnfnt\)Phys. Lett. B](#) **4**,09, 344 (1997); F. Larios and F. Penunuri, *J. Phys. G* **30**, 895 (2004); J. Cao *et al.*, [\(jnfnt\)Phys. Rev. D](#) **7**,0, 114035 (2004); O. Cakir *et al.*, *Eur. Phys. J. C* **70**, 295 (2010);
- [like-sign top-th2]** Yu. P. Gouz and S. R. Slabospitsky, [\(jnfnt\)Phys. Lett. B](#) **4**,57, 177 (1999).
- [like-sign top-th3]** S. K. Gupta, arXiv:1011.4960 [hep-ph].
- [like-sign top-ep1]** T. Aaltonen *et al.* [CDF Collaboration], *Phys. Rev. Lett.* **102**, 041801 (2009);
- [hexg]** X. G. He and G. Valencia, [\(jnfnt\)Phys. Rev. D](#) **6**,6, 013004 (2002); [\(jnfnt\)Phys. Rev. D](#) **6**,8, 033011 (2003).
- [cross section]** T. Aaltonen *et al.* [The CDF Collaboration], [\(jnfnt\)Phys. Rev. D](#) **8**,2, 052002 (2010);
- [mtt]** T. Aaltonen *et al.* [CDF Collaboration], [\(jnfnt\)Phys. Rev. Lett.](#) **1**,02, 222003 (2009).
- [pdg]** C. Amsler *et al.*, Particle Data Group, [\(jnfnt\)Phys. Lett. B](#) **6**,67, 1 (2008).
- [cteq]** J. Pumplin *et al.*, *JHEP* 0602, 032 (2006).
- [k-factor]** M. Cacciari *et al.*, *JHEP* 0809, 127 (2008); S. Moch and P. Uwer, [\(jnfnt\)Phys. Rev. D](#) **7**,8, 034003 (2008); N. Kidonakis and R. Vogt, [\(jnfnt\)Phys. Rev. D](#) **7**,8, 074005 (2008);
- [tug]** V. M. Abazov *et al.* [D0 Collaboration], [\(jnfnt\)Phys. Lett. B](#) **6**,93, 81 (2010).
- [tur]** S. Chekanov *et al.* [ZEUS Collaboration], [\(jnfnt\)Phys. Lett. B](#) **5**,59, 153 (2003).
- [tuz]** T. Aaltonen *et al.* [CDF Collaboration], *Phys. Rev. Lett.* **101**, 192002 (2008).
- [fcnc-susy]** See, e.g., C. S. Li, R. J. Oakes, J. M. Yang, [\(jnfnt\)Phys. Rev. D](#) **4**,9, 293 (1994); G. Couture, C. Hamzaoui, H. Konig, [\(jnfnt\)Phys. Rev. D](#) **5**,2, 1713 (1995); J. L. Lopez, D. V. Nanopoulos, R. Rangarajan, [\(jnfnt\)Phys. Rev. D](#) **5**,6, 3100 (1997); J. M. Yang, B. L. Young, X. Zhang, [\(jnfnt\)Phys. Rev. D](#) **5**,8, 055001 (1998); J. M. Yang, C. S. Li, [\(jnfnt\)Phys. Rev. D](#) **4**,9, 3412 (1994); J. Guasch, J. Sola, [\(jnfnt\)Nucl. Phys. B](#) **5**,62, 3 (1999); G. Eilam *et al.*, [\(jnfnt\)Phys. Lett. B](#) **5**,10, 227 (2001); C. S. Li, L. Yang, L. Jin, [\(jnfnt\)Phys. Lett. B](#) **5**,99, 92 (2004); Z. Heng *et al.*, [\(jnfnt\)Phys. Rev. D](#) **7**,9, 094029 (2009); J. Cao *et al.*, [\(jnfnt\)Phys. Rev. D](#) **7**,9, 054003 (2009); [\(jnfnt\)Phys. Rev. D](#) **7**,5, 075021 (2007); [\(jnfnt\)Phys. Rev. D](#) **7**,4, 031701 (2006); [\(jnfnt\)Nucl. Phys. B](#) **6**,51, 87 (2003).
- [fcnc-tc]** X. Wang *et al.*, [\(jnfnt\)Phys. Rev. D](#) **5**,0, 5781 (1994); G. Lu *et al.*, [\(jnfnt\)Phys. Rev. D](#) **6**,8, 015002 (2003); J. Cao *et al.*, [\(jnfnt\)Phys. Rev. D](#) **7**,6, 014004 (2007); [\(jnfnt\)Phys. Rev. D](#) **6**,7, 071701 (2003); H. J. Zhang, [\(jnfnt\)Phys. Rev. D](#) **7**,7, 057501 (2008).
- [fcnc-lh]** X.-F. Han, L. Wang, J. M. Yang, arXiv:0903.5491; X. Wang, *et al.*, [\(jnfnt\)Nucl. Phys. B](#) **8**,07, 210 (2009); Y. Zhang, G. Lu, X. Wang, arXiv:1011.0552;
- [wulei]** J. Cao, L. Wu, J. M. Yang, arXiv:1011.5564 [hep-ph].
- [enery resolution]** G. Aad *et al.* [The ATLAS Collaboration], arXiv:0901.0512 [hep-ex].
- [loop]** B. A. Kniehl, *Phys. Rep.* **240**, 211 (1994).

[Hahn] T. Hahn, M. Perez-Victoria, Comput. Phys. Commun. **118**, 153 (1999); T. Hahn, Nucl. Phys. Proc. Suppl. **135**, 333 (2004).